

Multi-objective optimization of pulsed gas metal arc welding process based on weighted principal component scores

Anderson P. Paiva · Sebastião C. Costa ·
Emerson J. Paiva · Pedro Paulo Balestrassi ·
João R. Ferreira

Received: 11 September 2008 / Accepted: 22 December 2009 / Published online: 2 February 2010
© Springer-Verlag London Limited 2010

Abstract Most welding processes present large sets of correlated quality characteristics. With this particularity in mind, we present a multi-objective optimization technique based on Principal Component Analysis (PCA) and response surface methodology (RSM). This two-fold technique utilizes PCA to factorize the original welding responses. The original responses—obtained through a Central Composite Design—are then replaced by the resulting principal component scores. The technique's advantage is that it reduces the data set and still considers the correlation among the responses. Quite often, however, the first principal component alone cannot explain the amount of variance—covariance structure of the welding responses. In this paper, we remedy this shortfall by proposing an objective function established in terms of the most significant principal component scores (weighted by their respective eigenvalues). Experimental results were obtained with a multiresponse pulsed gas metal arc welding process. These results, when compared with other strategies of multiresponse combination, verify the adequacy of our proposed approach.

Keywords Multi-objective optimization · Response surface methodology (RSM) · Principal Component Analysis (PCA) · Pulsed gas metal arc welding (P-GMAW)

Abbreviations and symbols

CCD	Central composite design
WMI	Weighted multivariate index
A	Weld bead area
H	Weld bead height
W	Weld bead width
R	Weld bead reinforcement
ξ	CCD design radius or axial distance
Σ	Covariance matrix of response random vector $Y^T = [Y_1, Y_2, \dots, Y_p]$
P	Weld bead penetration
p	Number of responses in a multivariate design
Y_p	p -th response of a multivariate data set
β	Model coefficient
PC_i	i -th principal component
e_i^T	Eigenvectors related to the i -th eigenvalue
Z	Standardized response data matrix
E	Matrix of the eigenvectors for the multivariate data set
λ_p	p -th eigenvalue of a data set
Λ_j	j -th Lagrange multiplier
R	Correlation matrix
n	sample size or number of experiments in a respective design
χ^2	Chi-square distribution
α	Significance level
r_{ij}	Pearson's correlation coefficient between response variables i and j
\bar{r}	Mean of the r_{ij} Pearson's correlation coefficients
μ	Gamma function
\bar{r}_ω	Mean of each line formed with the off-diagonal elements of R

A. P. Paiva · S. C. Costa · E. J. Paiva · P. P. Balestrassi (✉) ·
J. R. Ferreira
Industrial Engineering Institute, Federal University of Itajuba,
Itajuba, Minas Gerais, Brazil
e-mail: pedro@unifei.edu.br

A. P. Paiva
e-mail: andersonppaiva@unifei.com.br

S. C. Costa
e-mail: sccosta@unifei.edu.br

E. J. Paiva
e-mail: emersonjpaiva@gmail.com.br

J. R. Ferreira
e-mail: jorofe@unifei.edu.br

ω	Rank of the correlation matrix R
I_K	Kulbach index
I_D	Divergence index
I_R	Redundancy index
K	Number of experimental factors duty cycle
PC_p	p -th significant principal component
x	Vector of the experimental parameters; $x^T = [x_1, x_2, \dots, x_k]$
ϕ	Convexity index; $\phi = H/W$
Ω	Experimental region
δ	Small perturbations
\bar{x}	Optimum of the perturbed problem
x^*	Local optimum
df	Degree of freedom
I_p	Peak welding current
I_b	Background welding current
f	Wire feed rate
ϕ	Convexity index (H/W)

1 Introduction

Optimization techniques are very powerful tools used in manufacturing and service industries. Researchers have directed their attention to the case when there is only one goal to optimize. However, in the real world, products and services have several characteristics, often conflictive among themselves, and choosing parameters that provide global optimization for more than one characteristic of interest is not an easy task. Also, when responses are correlated, the individual analysis of each output is an unsatisfactory alternative. In fact, if one ignores the correlations between the outputs, one achieves an unreliable setting that improves the quality of all the responses simultaneously [1, 2]. Practitioners wanting to obtain an approximately true relationship between input and output variables, generally employ Design of Experiments (DOE) and regression techniques. These techniques, however, can be greatly influenced by the correlations, causing model instability, over fitting, and errors of prediction [3].

The welding optimization literature frequently reveals correlation among responses. It happens mainly when the weld bead geometry and shape are considered in the same analysis. Murugan and Gunaraj [4], for example, studied five responses of a submerged arc welding (SAW) process, considering penetration (P), reinforcement (R), and width (W). They also calculated shape relationships considering the penetration size factor (W/P) and the reinforcement form factor (W/R). When they then considered, at the same time, the geometric characteristics and their relationships with W/P and W/R , the response data set revealed a strong correlation structure.

Many other examples from welding literature illustrate this tendency. Kannan and Murugan [5] studied a flux-cored arc welding with eight responses. All of them presented significant correlations among each pair of response variables. Pearson's correlation coefficient equal to 0.88 was seen to be established between penetration (P) and dilution (D), and 0.81 was observed between reinforcement (R) and bead width (W). Along the same lines, strong and significant correlation is seen in processes like SAW [6], resistance spot welding [7], and laser welding [8]. Such correlation in these welding processes can also be observed in many applications of DOE with correlated responses. Yet, their influence over the estimated parameters of the response models is generally negligible.

We can handle multiresponse optimization of welding problems in two ways. We can gather the weighted sum of all the outputs into a single objective function [9, 10] or we can optimize one of the targets and enforce the constraints on the other targets [11]. If we focus on the first approach, we find that most researchers employ overall indices that convert the multiple quality characteristics into a single function. This function, in turn, must be optimized [12, 13]. Most choose to ignore the influence of the correlation structure that exists in the original data set. Such choice may result in non-conclusive results.

Several researchers, in addressing the correlation influence in multiresponse optimization, have used a Principal Component Analysis (PCA)-based approach [14, 15, 30, 31]. Let us suppose we are optimizing a manufacturing process with correlated responses. For an objective function, we would generally use the uncorrelated linear combination represented by the principal component scores of the original responses [14]. We would collect the multiresponse data sets to be factorized in PCA using a DOE technique like Taguchi arrays [14–18] or RSM [19]. While effective, the trade-off with this approach is that the first principal component score is not always enough to explain most of the variance–covariance structure.

This paper, in response to these concerns, proposes an optimizing strategy for correlated multiresponse processes. It is a strategy that aggregates all the significant principal component scores weighted by their respective eigenvalues. We call such an objective function the weighted multivariate index (WMI). It is a good counter-measure to a weakly performing first principal component that poorly represents the original data set [18–20].

In the following sections, this paper details the weighted multivariate optimization method.

2 The weighted multivariate response surface approach

A statistical technique, PCA summarizes, in a few uncorrelated components, common patterns of variation among response variables. It uses the factorization of a variance–covariance (Σ) or correlation (R) matrix associated with the random vector $Y^T = [Y_1, Y_2, \dots, Y_p]$, to produce pairs of eigenvalues (λ_i) eigenvectors (e_i) and an uncorrelated linear combination $PC_i = e_i^T Y$, with $i=1, 2, \dots, p$. The original data set may be then replaced by the uncorrelated linear combinations in the form of principal component score (PC_{score}). If Z is the standardized data matrix and E is the eigenvectors matrix of the multivariate set, then the PC_{score} can be written as [24]:

$$PC_{score} = [Z] \times [E] \tag{1}$$

To verify a sufficient number of principal component scores which may replace the original responses, there is a variety of stopping rules. Most popular is Kaiser’s criteria by which the researcher keeps only the principal components whose eigenvalues are greater than one [24]. At the same time the researcher considers an explained cumulative variance greater than 80%. It is also possible to employ χ^2 test [25–27] defined in Eq. 2, with $p(p - 1)/2$ degrees of freedom, to verify if the higher eigenvalues are significant. The null hypothesis is that all variables are uncorrelated.

$$\chi^2 = - \left[n - \frac{1}{6} (2p + 11) \right] \ln|R| \tag{2}$$

To test if the eigenvalue of the second principal component is different from the remaining ones [28], we may employ Eq. 3, approximately distributed as a χ^2 , with $(p + 1)(p - 2)/2$ degrees of freedom. By rejecting the null hypothesis, we assume that the second eigenvalue is also significant and must be kept to compose the multivariate index.

$$\chi^2 = \frac{n - 1}{1 - \bar{r}} \sum_{j \neq i=1}^p \sum_{i \neq j=1}^p (r_{ij} - \bar{r})^2 - \mu \sum_{k=1}^p (\bar{r}_\omega - \bar{r})^2 \tag{3}$$

with

$$\bar{r} = \frac{2}{p(p - 1)} \sum_{i=\omega+1}^p \sum_{j=1}^p r_{ij}, \tag{4}$$

$$\mu = \frac{(p - 1)^2 [1 - (1 - \bar{r})^2]}{p - (p - 2)(1 - \bar{r})^2}, \bar{r}_\omega = \frac{1}{(p - 1)} \sum_{\substack{i=1 \\ i \neq j}}^p r_{i\omega}$$

For both cases (Eqs. 2 and 3), the null hypothesis is rejected when $p < 0.05$.

The dependence structure may also be assessed using Kulbach index (I_K), divergence index (I_D), and redundancy index (I_R) [29], all of them based on the correlation matrix R . Such statistics can be written as:

$$I_K = -\frac{1}{2} \ln|R| = -\frac{1}{2} \sum_{i=1}^p \ln(\lambda_i) \tag{5}$$

$$I_D = \frac{1}{2} \text{trace}(R^{-1}) = \sum_{i=1}^p \left[\frac{(1 - \lambda_i)}{2\lambda_i} \right] \tag{6}$$

$$I_R = \sqrt{\frac{\|R\|^2 - p}{p(p - 1)}} = \sqrt{\frac{\left(\sum_{i=k+1}^p \sum_{j=1}^p r_{jK}^2 \right) - p}{p(p - 1)}} \\ = \sqrt{\frac{\left(\sum_m \lambda_m \right) - p}{p(p - 1)}} \tag{7}$$

Considering the eigenvalues of the correlation matrix as a set of weights, we can write the WMI as $\sum_{p=1}^r [\lambda_p(PC_p)]$.

Applying the ordinary least squares (OLS) algorithm for WMI, we obtain a second-order polynomial such as Eq. 8.

$$Y = \beta_0 + \sum_{i=1}^K \beta_i x_i + \sum_{i=1}^K \beta_{ii} x_i^2 + \sum_{i < j}^K \beta_{ij} x_i x_j + \varepsilon \tag{8}$$

and the multivariate optimization system may be established as:

$$\text{Maximize } WMI = \sum_{p=1}^r [\lambda_p(PC_p)] \tag{9}$$

$$\text{Subject to : } x^T x \leq \xi^2 \tag{10}$$

The assumption of maximization described in Eq. 9 is established supposing that the desired optimization direction for each original response is positively correlated with the multivariate index. These may be defined by analyzing the correlation between a WMI and each original response. For positive correlation between WMI and an original response, both functions will have the same direction of optimization. If the correlation between WMI and a response is negative, the maximization of WMI implies the minimization of the response and vice versa. Inspection of the eigenvectors will reveal the kind of relationship that exists between the i -th principal component score and the original responses.

A potential difficulty in optimizing a multivariate response generally occurs due to conflicting minima and maxima in a group of variables that, for instance, must be simultaneously maximized. In this case, optimizing the principal component equation will benefit some responses but impede others [19]. To avoid this aspect of the multivariate approach, a particular solution can be proposed using the following two-step strategy:

1. Start the solution using a one-dimensional optimization of each response separately.
2. The optimum achieved in Step 1 for all the responses will be considered as targets for a multivariate nominal-the-best problem. This approach is discussed in Paiva et al. [31].

Although this strategy seems to be adequate, we will not employ it here since the responses do not present any conflict with the principal component optimization in this specific case.

To solve the Nonlinear Programming (NLP) problem of Eqs. 9 and 10, the practitioner can use any optimization algorithm. We adopt in this work, the generalized reduced gradient (GRG), one of the most robust and most efficient methods for constrained NLP optimization [23, 32].

3 Experimental procedure and data analysis

To accomplish the aims of this paper, we chose a pulsed gas metal arc welding (P-GMAW) [34] process. It is a case study that illustrating our method's applicability presents a particular correlation structure among the quality characteristics. To optimize the output variables that affect the P-GMAW weld quality characteristics, we adopt the multivariate response surface approach. We obtained these characteristics according to a fully rotatable central composite design (CCD; Table 2) for four welding parameters (Table 1), with seven center points. These center points' runs provide an internal estimate of error (pure error) and contribute toward the estimation of quadratic terms [21, 41]. In other words, when we use CCD, we obtain the significance of the terms by using the mean square error) from center point's replications (the ANOVA within

variation). This process allows us to calculate the ANOVA critical t , F , and p values. In this case, it was not necessary to replicate the entire design.

The P-GMAW process presents many particularities. These mainly relate to avoiding the drawbacks of globular mode. At the same time, the process achieves the benefits of spray transfer used in the traditional gas metal arc welding (GMAW) process. The P-GMAW is characterized by a pulsing of current between a low-level background current and high-level peak current. The current pulses in such a way that an average current is always below the threshold level of spray transfer. The background current is used to maintain arc when peak currents are long enough to make sure there is detachment of the molten droplets [34].

In the traditional GMAW process, globular metal transfer mode occurs when the system is operating in low welding current. As the current increases, the globular mode changes to spray mode. The modular mode is characterized by the periodic formation of big droplets at the outermost of the electrodes. These droplets, due to gravitational force, detach into the weld pool. The formation of big droplets causes the process to suffer from arc instability and a lack of control over the molten droplets. While the spray mode offers a high deposition rate, for some material, its minimum current is too high. Further drawbacks include its large heat input and the wide bead [34].

To establish a highly reliable P-GMAW process, we must to find out the important parameters and levels that are connected to the P , W , and A . These must be maximized, while H and ϕ must be minimized. The necessary information to build a second-order model was obtained and is included in Table 2. The convexity index ϕ was determined using the expression $\phi = H/W$.

To run the experimental design, we used an electric power source running on a pulsed-mode current of imposition. Such a source normally allows more flexibility to adjust for the parameters. Connected to the equipment was a mechanical tractor used to move the attached torch at the adjustable welding speed. All welding tests were performed using a weld-bead-on-plate technique. An AWS ER 70S-6 wire with a diameter of 1.2 mm was used. Its base material type was ABNT 1045 with $120 \times 40 \times$

Table 1 Process parameters

Parameters	Symbol	Units	Levels				
			-2	-1	0	1	2
Peak current	I_p	Ampere	245	280	315	350	385
Background current	I_b	Ampere	55	70	85	100	115
Duty cycle	k	%	35	40	45	50	55
Wire feed rate	f	m/min.	4.5	5	5.5	6	6.5

Table 2 Welding parameters and responses for the CCD design

Parameters					Responses					Principal components		
N	I_p	I_b	k	f	P , mm	H , mm	W , mm	ϕ	A , mm ²	PC_1	PC_2	WMI
1	280	70	40	5	1.60	2.87	7.70	37.20	20.70	-1.031	1.677	-0.9088
2	350	70	40	5	1.60	2.90	6.60	44.40	19.00	-2.627	1.085	-6.4294
3	280	100	40	5	1.70	2.80	7.00	39.60	20.70	-1.556	1.703	-2.4407
4	350	100	40	5	1.87	3.10	6.30	43.00	18.70	-2.339	0.366	-6.4996
5	280	70	50	5	1.90	3.00	7.30	41.60	23.20	-0.927	0.491	-2.1302
6	350	70	50	5	1.66	3.70	6.00	52.50	20.90	-3.366	-2.941	-13.8241
7	280	100	50	5	1.96	2.90	8.10	35.50	21.50	-0.021	1.564	1.9560
8	350	100	50	5	1.90	3.30	7.90	38.00	22.80	-0.2543	-0.333	-1.1872
9	280	70	40	6	1.20	3.48	7.30	46.00	20.70	-2.619	-1.369	-9.5707
10	350	70	40	6	1.90	3.10	8.10	38.90	24.90	0.064	0.194	0.4430
11	280	100	40	6	1.22	3.50	7.20	48.30	23.00	-2.547	-1.859	-9.9904
12	350	100	40	6	1.95	3.10	8.60	35.90	27.00	1.019	0.252	3.3631
13	280	70	50	6	2.10	3.20	8.10	39.20	25.70	0.427	-0.342	0.8307
14	350	70	50	6	2.08	3.20	8.70	36.40	25.10	0.949	-0.025	2.7951
15	280	100	50	6	1.96	3.00	8.40	36.40	25.50	0.646	0.735	2.8727
16	350	100	50	6	2.30	3.20	9.20	28.50	28.40	2.772	0.276	8.6149
17	245	85	45	5.5	1.85	3.00	8.80	40.00	29.00	0.889	0.158	2.8555
18	385	85	45	5.5	2.29	3.12	8.10	38.10	27.00	0.967	-0.101	2.7525
19	315	55	45	5.5	1.79	2.91	8.50	34.50	21.70	0.117	1.643	2.4672
20	315	115	45	5.5	2.20	3.00	9.30	29.10	26.00	2.288	1.269	8.4578
21	315	85	35	5.5	1.42	3.00	7.60	39.50	22.30	-1.323	0.862	-2.8297
22	315	85	55	5.5	2.10	3.40	9.20	32.70	28.30	2.098	-0.797	5.2226
23	315	85	45	4.5	1.80	2.80	6.00	46.40	17.40	-3.144	1.397	-7.5685
24	315	85	45	6.5	2.02	3.20	8.10	39.50	26.80	0.444	-0.453	0.7391
25	315	85	45	5.5	2.60	3.25	8.80	36.20	30.70	2.526	-0.84	6.4451
26	315	85	45	5.5	2.10	3.30	8.10	40.70	27.60	0.557	-1.036	0.3245
27	315	85	45	5.5	2.20	3.30	8.70	38.10	28.90	1.491	-0.94	3.2292
28	315	85	45	5.5	2.50	3.10	8.00	38.80	26.90	1.109	-0.118	3.1535
29	315	85	45	5.5	2.32	3.35	7.80	42.00	28.00	0.608	-1.437	-0.0406
30	315	85	45	5.5	2.40	3.30	8.30	39.80	30.10	1.525	-1.253	2.9270
31	315	85	45	5.5	2.40	3.10	8.40	36.90	25.90	1.258	0.17	3.9704

6 mm. The shielding gas was a mixture of Argon and 25% CO₂ with a constant flow of 15 l/min. The welding speed was kept constant at 40 cm/min, and for all the tests the standoff was 22.5 mm. The welding parameters and levels are described in Table 1 and the experimental design in Table 2. According to Ghosh et al. [35], the duty cycle (k) was obtained using Eq. 13, where t_p is the peak time, fixed at 4 ms, and t_b the background time, varying according to the desired level.

$$k = \frac{t_p}{t_p + t_b} \tag{13}$$

After welding, all test specimens were cross-sectioned, polished, chemically attacked, and then the geometric charac-

teristics of P , H , W , and A were determined. The convexity index ϕ was determined using the expression $\phi = H/W$.

The first two principal components also shown in Table 2 were obtained by applying Eq. 1 to the original welding characteristics. Hence, while the principal component scores PC_1 and PC_2 were determined, the OLS algorithm was applied to create the multivariate objective functions. These functions depend on the PCA eigenanalysis and the multivariate indices. By observing the results shown in Table 3, we may conclude that the multivariate approach is an adequate option for the welding data. Table 3 shows the results of Bartlett’s and Lawley’s tests, according to Eqs. 2, 3, and 4. As the test statistics are greater than the critical values ($p < 5\%$), we reject the null hypothesis; this implies that the first two principal components are significant.

Table 3 Tests and indexes for determination of non-trivial axes in the PCA analysis

Test type	Critical value	Test value	df	p values
Bartlett	18.307	134.210	10	0.000
Lawley	16.920	93.156	9	0.000
Indexes		I_K	I_D	I_R
		2.440	25.756	0.007

The indices I_K , I_D , and I_R , established according to Eqs. 5, 6, and 7, also reveal a high correlation among the welding characteristics. This result means that the variance–covariance structure really supports a multivariate approach. Table 4 shows that, taken together, the two principal components represent 85.5% of the variation in the responses. PC_1 is capable of explaining only 59.6% of the total variation. This is considered a poor explanation. In addition, we can see that the first and the second eigenvalues are greater than one. Based on these statistical tests and indices, we might postulate that, to form the WMI, only the first two PC 's must be chosen. The WMI values reported in Table 2, obtained according to Eq. 9, becomes $WMI = \lambda_1(PC_1) + \lambda_2(PC_2)$ considering the first and second eigenvalues equals to 2.98 and 1.29, according to Table 4. Then the multivariate objective function can be written as:

$$\begin{aligned}
 WMI = & 2.845 + 0.267I_p + 1.556I_b + 1.995k + 1.968f \\
 & - 0.597I_p^2 + 0.066I_b^2 \\
 & - 0.998k^2 - 2.146f^2 + 1.067I_pI_b - 1.305I_pk + 3.459I_pf \\
 & + 1.477I_bk - 0.297I_bf + 1.857kf
 \end{aligned}
 \tag{14}$$

Figure 1 represents the multivariate objective function obtained with WMI criteria as a function of the variables I_p and k . Notice, in terms of the process parameters, the nonlinear behavior of WMI; the function is concave, and the stationary point is a maximum. The optimization

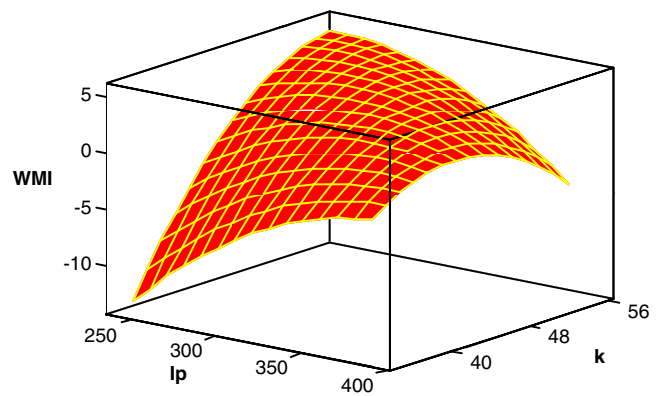


Fig. 1 WMI surface plot as a function of I_p and k

direction of WMI can be defined observing the correlation among the principal components and the original data set, represented by the eigenvectors in Table 4. The relationship between eigenvectors and Pearson's correlation coefficients is straightforward [24]. Some findings from this relationship are: (1) a high positive correlation between PC_1 and the responses P , W , and A ; (2) a high negative correlation between PC_1 and ϕ , and (3) a high negative correlation between PC_2 and H . To improve the present welding process, as cited above, the responses P , W , and A must be maximized while H and ϕ must be minimized. From analysis of the correlation between the principal components and the responses, we can conclude that by maximizing PC_1 , the responses P , W , and A will be maximized while ϕ will be minimized; by maximizing PC_2 , H will be minimized. PC_1 is not enough to explain most of the variance–covariance structure among the five original responses. We can employ, to obtain a proper solution, the maximization of WMI, which keeps the same kind of correlation with the original data set and PC_1 . Since WMI is concave, the stationary point is a maximum and the optimization of all desired responses can be achieved (Fig. 1). Using the GRG method to solve the optimization problem, the spherical constraints will be imposed on the

Table 4 Principal component analysis of the original P-GMAW responses

	Principal components				
	PC_1	PC_2	PC_3	PC_4	PC_5
Eigenvalues	2.9775	1.2957	0.5165	0.1856	0.0246
Proportion	0.5960	0.2590	0.1030	0.0370	0.0050
Accumulated	0.5960	0.8550	0.9580	0.9950	1.0000
Responses	Eigenvectors				
P	0.4680	-0.0730	0.7900	-0.3190	-0.2250
H	0.0140	-0.8440	-0.2630	-0.4650	0.0400
W	0.5420	0.0450	-0.4590	0.1340	-0.6900
ϕ	-0.4800	-0.4040	0.3060	0.5030	-0.5090
A	0.5070	-0.3410	0.0590	0.6400	0.4610

factor’s levels, forcing the values that optimize the responses to fall into the experimental interval $-\xi \leq x_i \leq +\xi$. For a CCD design with four factors, $\xi=2$ [21].

As can be observed in Table 2, the CCD was used to obtain the original set of responses (P , H , W , A , and ϕ). These responses were factorized using PCA, and the first and second principal component scores were stored. Using the first and second eigenvalues as weights, the principal components were aggregated into WMI. Tables 5 and 6 present the second-order model and the ANOVA, respectively, obtained for the processed response WMI.

To assess the significance of each coefficient of the model, a two-sided t test is used. For the purposes of the analysis, the null hypothesis is stated as equality between the response mean obtained in the levels +1 or -1 of each parameter, such as $H_0 : \mu_{(-1)} = \mu_{(+1)}$. Therefore, rejecting the null hypothesis means that the factor is significant. If the p value is less than the significance level, the null hypothesis must be rejected. Table 7 presents the significant parameters for all responses focused on in this work. Additionally, Table 5 also presents the significance of the entire model. Since $p < 5\%$, the full quadratic model is significant. The linear, square, and interaction terms of the full quadratic model are also individually assessed. The null hypothesis in this case is that the coefficient of a specific parameter is equal to zero, such as $H_0: \beta_i=0$ against the alternative hypothesis $H_0: \beta_i \neq 0$. In this case, all the p values are less than 5%, indicating that at least one of linear effects (and parameters) is significant.

When refining the model, a common approach is to remove any nonsignificant terms, since the hierarchy principle is not being violated, from the full model. This hierarchical model-building principle [21] promotes an

Table 5 Second-order model for WMI

Term	Coef	SE coef	T	p values
Constant	2.858	1.037	2.756	0.014
I_p	0.269	0.560	0.480	0.638
I_b	1.561	0.560	2.787	0.013
k	2.003	0.560	3.575	0.003
f	1.977	0.560	3.529	0.003
I_p^2	-0.600	0.513	-1.169	0.259
I_b^2	0.065	0.513	0.126	0.901
k^2	-1.002	0.513	-1.952	0.069
f^2	-2.155	0.513	-4.199	0.001
$I_p I_b$	1.071	0.686	1.561	0.138
$I_p k$	-1.307	0.686	-1.906	0.075
$I_p f$	3.468	0.686	5.055	0.000
$I_b k$	1.480	0.686	2.158	0.046
$I_b f$	-0.297	0.686	-0.434	0.670
$k f$	1.861	0.686	2.713	0.015

Table 6 Anova for WMI

Source	df	SS	MS	F0	p values
Regression	14	737.44	52.675	6.99	0.000
Linear	4	250.24	62.561	8.31	0.001
Square	4	157.17	39.293	5.22	0.007
Interaction	6	330.03	55.005	7.30	0.001
Residual error	16	120.49	7.531		
Lack-of-fit	10	91.34	9.134	1.88	0.227
Pure error	6	29.15	4.859		
Total	30	857.94			

internal consistency in the model and suggests that when a particular polynomial term is included in a model, all lower-order polynomial terms should also be included, even those terms that do not exhibit significance individually.

For this experimental study, the nonlinear response surface is adequate, indicated by the low p values for the regression terms and a p value of 0.227 for the lack-of-fit (Table 6). Moreover, since higher-order terms, like interaction, are significant, the lower ones must be part of the model. For example, if the interaction $I_p f$ is significant, then the peak current (I_p) must be kept in the model, despite (I_p) not being important to the WMI explanation. Table 7 shows the second-order model for PC_1 , WMI, and also for each welding bead characteristic. In spite of some nonsignificant terms being detected, its exclusion from the complete model has increased the error S and reduced the R^2_{adj} . Figure 2 presents the accuracy of the predicted WMI and the measured WMI.

Considering the full quadratic model of WMI as a multivariate objective function described by Eq. 9 and applying the spherical constraint from Eq. 10, the optimal settings for the design factors of the P-GMAW welding process in coded units are [0.8565, 1.2988, 0.9068, 0.8701] or in uncoded units, $I_p=344.9$ A, $I_b=104.5$ A, $k=49.5\%$, and $f=5.9$ m/min. The optimal settings were obtained using a GRG nonlinear optimization routine available in Excel Solver®.

To compare the obtained results using WMI, we propose a prioritized nonlinear constrained optimization and a desirability approach. Using the fitted equations of the welding outputs shown in Table 7 as constraints and choosing the weld bead penetration (P) as an objective function, we can write the optimization system as:

$$\text{Maximize } P = b_0 + \nabla f(x)^T + \frac{1}{2} x^T [\nabla^2 f(x)] x \tag{15}$$

$$\text{Subject to : } 3 \leq H \leq 3.5 \tag{16}$$

$$8 \leq W \leq 10 \tag{17}$$

Table 7 Ordinary least squares coefficients for original responses, PC_1 and WMI

Model term	Regression coefficients (full quadratic model)							
	P	H	W	φ	A	PC_1	WMI	
Constant	2.36000	3.24286	8.30000	38.9286	28.3000	1.29657	2.84546	
I_p	0.10417	0.04542	-0.04583	-0.4167	0.0750	0.16678	0.26714	
I_b	0.06833	-0.01542	0.18750	-1.7417	0.6667	0.46636	1.55636	
k	0.17417	0.06042	0.33750	-1.6167	1.2667	0.77920	1.99496	
f	0.04000	0.08375	0.53750	-1.5000	2.1500	0.83376	1.96822	
I_p^2	-0.09375	-0.03019	-0.05312	0.4658	-0.3792	-0.25958	-0.59745	
I_b^2	-0.11250	-0.05644	0.05937	-1.3467	-1.4167	-0.19106	0.06648	
k^2	-0.17125	0.00481	-0.06563	-0.2717	-1.0542	-0.39484	-0.99799	
f^2	-0.13375	-0.04519	-0.40313	1.4408	-1.8542	-0.82927	-2.14643	
$I_p I_b$	0.04625	0.00938	0.14375	-1.4125	0.4125	0.34407	1.06718	
$I_p k$	-0.09875	0.10937	-0.03125	0.7250	-0.2000	-0.24347	-1.30495	
$I_p f$	0.11750	-0.12562	0.43125	-3.3875	0.9500	0.87181	3.45943	
$I_b k$	-0.00375	-0.05313	0.25625	-1.9750	-0.0500	0.32941	1.47711	
$I_b f$	-0.03250	0.01188	-0.03125	0.5125	0.4750	-0.04455	-0.29698	
$k f$	0.09500	-0.11313	0.09375	-2.0000	-0.0125	0.36806	1.85729	
R^2 (adj.)	83.2%	71.0%	72.2%	80.7%	75.5%	78.7%	73.7%	

$$20 \leq \phi \leq 26.5 \tag{18}$$

$$25 \leq A \leq 30 \tag{19}$$

$$I_p^2 + I_b^2 + k^2 + f^2 \leq 4.00 \tag{20}$$

where: $\mathbf{x}=[I_p, I_b, k, f]$, b_0 is the regression constant term, $\nabla f(\mathbf{x})^T$ is the gradient of the objective function corresponding to the first-order regression coefficients and $\nabla^2 f(\mathbf{x})^T$ is the Hessian matrix, formed by the quadratic and interaction terms of the estimated model of P . By using past data, we established the upper and lower bounds cited in Eq. 19. We

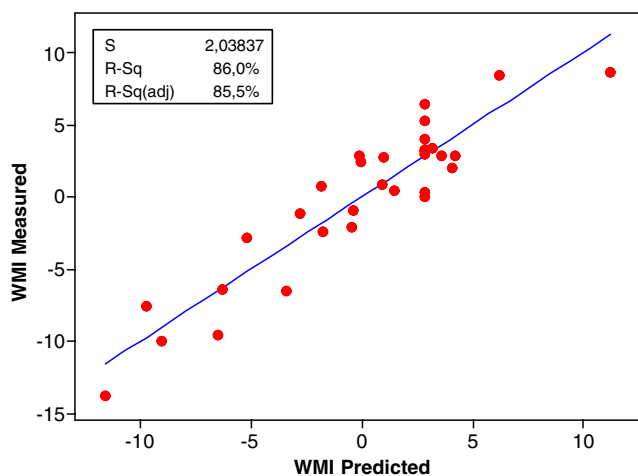


Fig. 2 Accuracy of the predicted WMI and the measured WMI

thought this previously gathered data would provide, in addition to a defect-free welded joint a feasible solution to the objective function. If WMI is adequate, we expect similar results. We chose as an objective function the weld bead penetration (P), as it was the most important response to the process. A similar approach can be applied by replacing the second-order model of P in Eq. 15 with H , W , ϕ , or A . However, it is not possible to affirm the achieved optimum will be the same.

Table 8 compares the three methods' results. Although the desirability method presents values for each response according to the proposed upper and lower bounds, the achieved optimum does not satisfy the spherical constraint. In this case, if the coded values to the parameters from the desirability approach are adopted [1.98, 0.58, 0.44, 2.00], the spherical constraint becomes $\mathbf{x}^T \mathbf{x} = 8, 47 \gg \xi^2$. Then, according to the imposed constraint, the desirability solution is not a reasonable alternative for handling the present problem. If the stationary point lies far from the design center, the prediction error will be higher [41]. Figure 3, comparing the results of the methods, presents the contour plots for WMI . Note that, as expected, the achieved optimum using the desirability method falls far from those points obtained with WMI and multiresponse optimization.

4 Sensitivity analysis of the welding parameters

In the optimization of the welding parameters, two possible strategies assess the sensitivity of WMI : (a) arbitrarily changing the constraint value (ξ^2) or (b) adopting, with

Table 8 Comparative results among methods

	<i>P</i>	<i>H</i>	<i>W</i>	ϕ	<i>A</i>	<i>I_p</i>	<i>I_b</i>	<i>k</i>	<i>f</i>
<i>WMI</i>	2.326	3.105	9.778	25.617	28.790	344.975	104.483	49.535	5.935
Multiple	2.373	3.115	9.705	26.500	29.405	354.333	101.732	48.909	5.969
Desirability	2.260	2.700	9.600	24.300	28.700	384.500	93.700	47.200	6.500
Upper bound	2.600	3.500	10.000	26.500	25.000	385.000	115.000	55.000	6.500
Lower bound	2.100	3.000	8.000	20.000	30.000	245.000	55.000	35.000	4.500

respect to each welding parameter, the partial derivatives of WMI. The first strategy was used in [6], considering a sensitivity analysis through a relaxing of the constraint values. Otherwise, the change in constraint value may be carried out by using the Lagrange multipliers concept. The Lagrange multipliers express the gradient at the optimum as a linear combination of the rows of the constraint matrix. The concept it is able to indicate the sensitivity of the optimal objective value to changes in the data [22]. A Taylor series can be used to obtain the approximation, assuming that the objective function is twice continuously differentiable and considering small perturbations (δ) in the right side of the constraints:

$$f(\bar{x}) = f(x^*) + \sum_{i=1}^m \delta_i \Lambda_{*i} \tag{21}$$

where x^* represents a local minimum, such as $x^* = \arg \min_x f(x)$.

In particular, Eq. 21 is valid if \bar{x} is the minimizer of the perturbed problem. If the right-hand side of the i -th constraint changes by δ_i , then the optimal objective value changes by approximately $\delta_i \Lambda_{*i}$. Hence Λ_{*i} represents the change in the optimal objective per unit changed in the i -th right-hand side. The Lagrange multipliers are also called in optimization software packages as “shadow prices” [22].

To write a nonlinear constrained optimization problem in an unconstrained form and considering the inequality constraints, it is plausible to consider the Lagrangian function as follows [36]:

$$L(x_i, \Lambda_j, s_j) = f(x_i) - \sum_{j=1}^n \Lambda_j \left\{ \sum_{i=1}^p a_{ji} x_i - b_j \right\} - \sum_{j=n+1}^m \Lambda_j \left\{ \sum_{i=1}^p a_{ji} x_i - b_j - s_j^2 \right\} \tag{22}$$

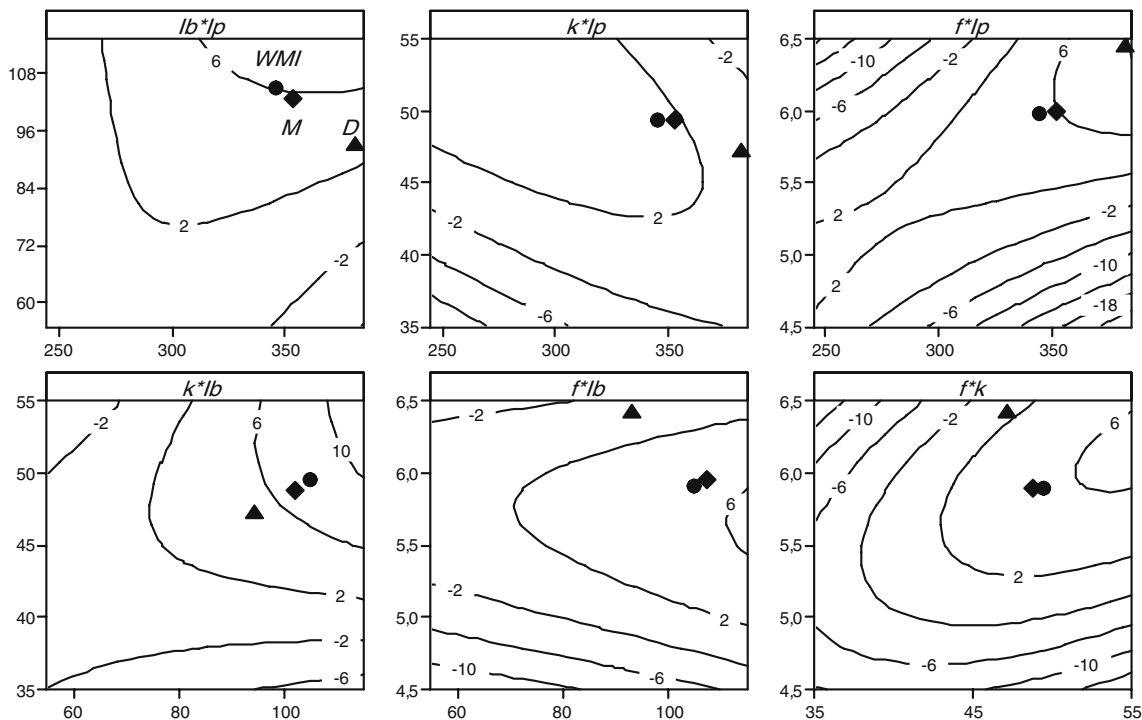


Fig. 3 Contour plots for *WMI* showing the results for three methods. Legend: *D* (filled triangle) desirability, *M* (filled diamond) multiple, *WMI* (filled circle) weighted multivariate index

where $\sum_{i=1}^p a_{ji}x_i - b_j$ are the constraints established in the optimization problem, and s_j are the slack variables used to transform the inequalities in equality constraints.

To solve Eq. 22, it is necessary to use the Karush–Kuhn–Tucker conditions [22], which can be done using the gradient of the Lagrangian function. The Lagrange multipliers can be determined using the optimization routine available in Microsoft Excel Solver [33]. The Lagrange multiplier obtained with the present data was $\Lambda_1=1.4345$ (referring to the WMI spherical constraint). Substituting this value in Eq. 22 it follows that:

$$WMI(\bar{x}) = WMI(x^*) + \sum_{i=1}^n \delta_i \Lambda^*_i = 11.467 + 1.4345 \cdot \delta_{(x^T x)} \tag{23}$$

The sensitivity analysis based on Eq. 23 can be obtained by varying the delta value. The relationship between WMI and δ , as can be seen, is a well-adjusted linear regression. Therefore, any positive or negative perturbation will change the objective function's proportionality. In this sense, adopting $\delta_{(x^T x)} > 0$, the spherical constraint is relaxed, while for $\delta_{(x^T x)} < 0$, the space of solution is diminished, probably forcing the optimization algorithm to find a more adequate optimum. For $\delta_{(x^T x)} = 0$, the constraint is, obviously, not altered.

Figure 4 shows the behavior of WMI for a perturbation range between $[-2, +2]$. Since the algorithm obeys a maximization routine, WMI increases for positive increments on the right side of the spherical constraints. Otherwise, a negative perturbation means the constraint is much more rigorous than in the relaxation case. As the problem is maximization, negative perturbations imply that the maximum obtained in the iterations, lies in the boundary imposed by the spherical constraint.

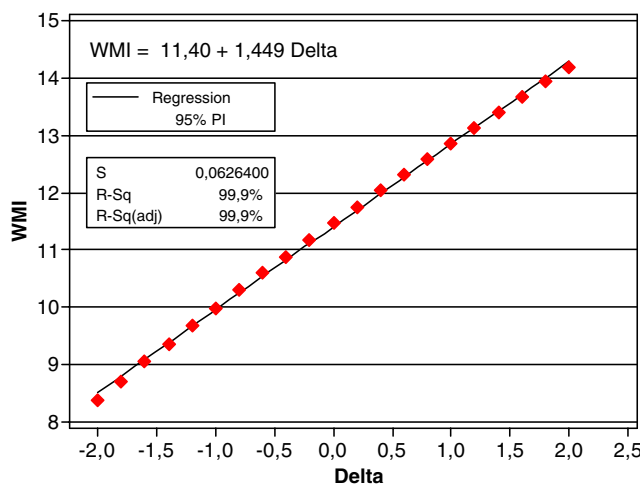


Fig. 4 Sensitivity analysis of WMI based on Lagrange multipliers concept

We can assess the sensitivity of a design objective function, very practically, by adopting the partial derivatives of an objective function with respect to each design variable [37, 38]. This analysis yields information, with respect to the design parameter, about the incremented or decremented tendency of the design objective function. A great number of researchers working with nonlinear objective functions for welding processes have employed this approach [37–40].

This study aims to predict how a small change in P-GMAW process parameters affects the tendency of the multivariate index WMI. As there is a strong correlation among the WMI and welding outputs, the WMI function's tendency ought to directly correspond to the original output set.

In this regard, considering the full quadratic model of WMI, the sensitivities with respect to $x=[I_p, I_b, k, f]$ are:

$$\frac{\partial f(I_p, I_b, k, f)}{\partial I_p} = 0.267 - 1.195I_p + 1.067I_b - 1.305k + 3.459f \tag{24}$$

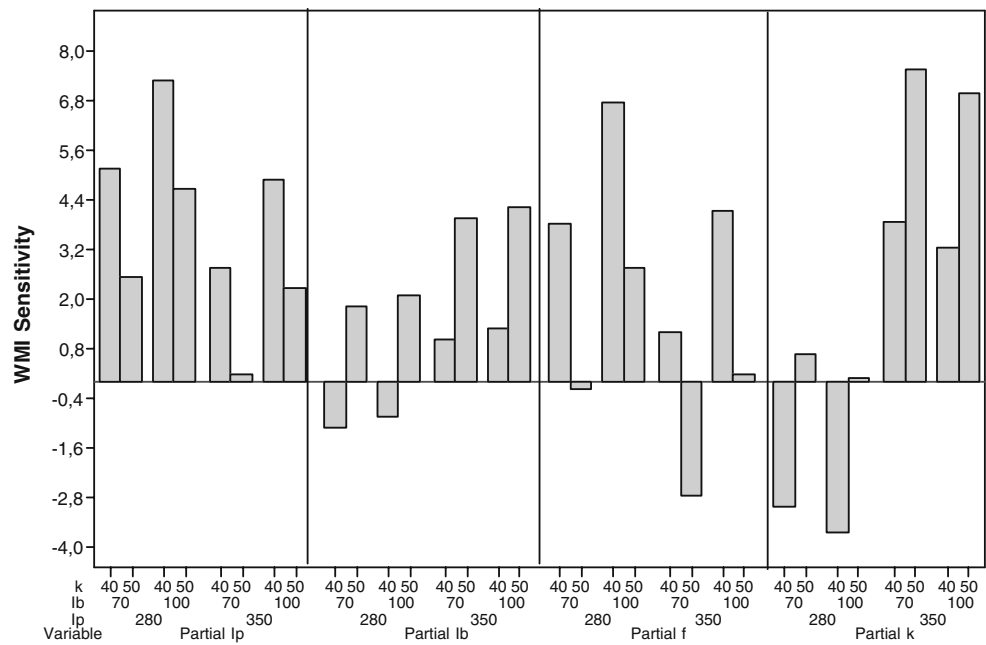
$$\frac{\partial f(I_p, I_b, k, f)}{\partial I_b} = 1.556 + 1.067I_p + 0.133I_b + 1.477k - 0.297f \tag{25}$$

$$\frac{\partial f(I_p, I_b, k, f)}{\partial k} = 1.995 - 1.305I_p + 1.477I_b - 1.996k + 1.857f \tag{26}$$

$$\frac{\partial f(I_p, I_b, k, f)}{\partial f} = 1.968 + 3.459I_p - 0.297I_b + 1.857k - 4.292f \tag{27}$$

The sensitivity analysis results are depicted in Fig. 5. The results correspond to simulated conditions for the process parameters. So that we could better understand the variation obtained by changing parameters, we developed simulated results of the four partial derivatives of WMI using the Eqs. 24 up to 27 and a coded 2^4 full factorial design. As shown in Fig. 5, from the Eq. 24, the peak current (I_p) sensitivity of WMI is negative. This sensitivity implies a decremental tendency, when I_p increases, in the predictive values of WMI. Since WMI is positively correlated with P , W , and A , large values of I_p also imply a reduced bead penetration (P), width (W), and area (A). Otherwise, the negative correlation observed among WMI, H and ϕ implies that the increase of I_p prompts the increase of H and ϕ . The wire feed rate (f) sensitivity of WMI (Eq. 25) is analogous to (I_p) sensitivity. Accordingly, the

Fig. 5 Sensitivity analysis of WMI considering f constant



background current (I_b ; Eq. 26) and duty cycle (k) sensitivities (Eq. 27) of WMI are positive. That is to say, as (I_b) and (k) values increase, P , W , and A also increase; H and ϕ values decrease.

To confirm the results and conclusions described above and depicted in Fig. 5, we repeated the sensitivity analysis for one of the original responses. Choosing penetration (P), for example, the sensitivities with respect to $x=[I_p, I_b, k, f]$ are:

$$\frac{\partial f(I_p, I_b, k, f)}{\partial I_p} = 0.104 - 0.187I_p + 0.046I_b - 0.098k + 0.118f \tag{28}$$

$$\frac{\partial f(I_p, I_b, k, f)}{\partial I_b} = 0.068 + 0.046I_p - 0.225I_b - 0.004k - 0.033f \tag{29}$$

$$\frac{\partial f(I_p, I_b, k, f)}{\partial k} = 0.174 - 0.099I_p - 0.004I_b - 0.343k + 0.095f \tag{30}$$

$$\frac{\partial f(I_p, I_b, k, f)}{\partial f} = 0.040 + 0.118I_p - 0.032I_b + 0.095k - 0.268f \tag{31}$$

As shown in Table 9, the correlation between WMI partial derivatives and P partial derivatives are all positives (the diagonal elements), meaning an increase in WMI corresponds to an increase in P . Figures 5 and 6 allow us to verify that, when the peak current (I_p) is 280 A, the WMI index and

P increase. When the background current (I_b) changes from 70 to 100 amperes, WMI and P increase significantly. WMI is evidently more sensitive to changes in the peak current (I_p) than to the penetration (P). The same can be observed with the parameter duty cycle (k). In both cases, a duty cycle of 50% increases, simultaneously, WMI and P . For the wire feed rate (f), the penetration is higher with 6 m/min than with 5 m/min. WMI is not, however, so sensitive to changes in the levels of this parameter. This comparison is clearly depicted in Fig. 6. All the graphical and statistical analyses in this work were done using Minitab 15®.

The present study illustrates that, in the sensitivity analysis, the correlation between the multivariate index and the original responses remains the same. We can extend this conclusion to the remaining welding responses and parameters of the P-GMAW process.

5 Conclusion

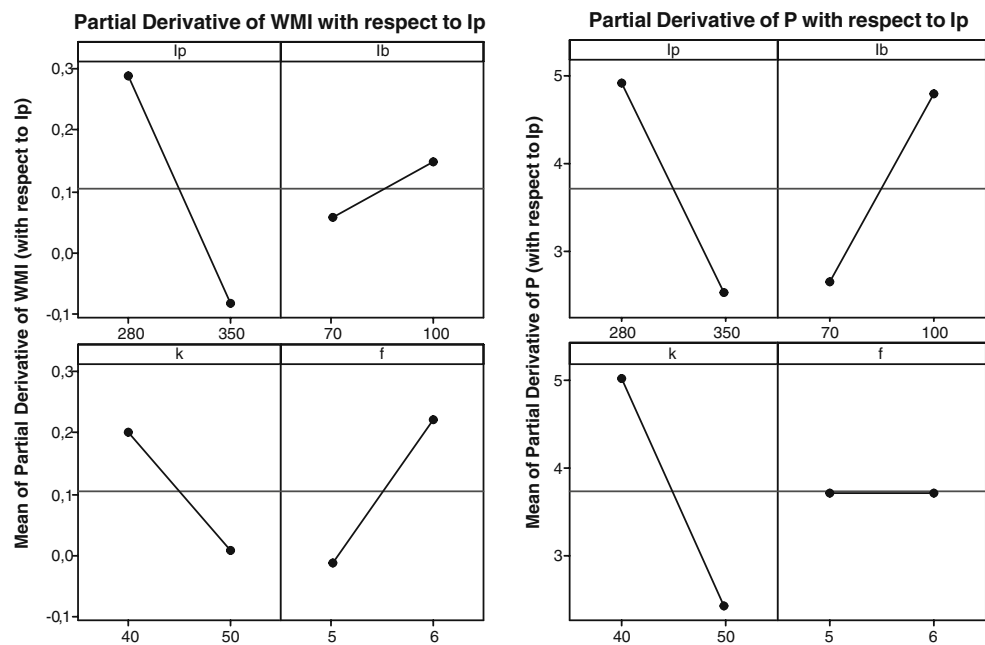
This work used a multi-objective optimization technique based on Principal Component Analysis to study a pulsed

Table 9 Correlation between sensitivity analysis of the welding parameters

	$\frac{\partial WMI}{\partial I_p}$	$\frac{\partial WMI}{\partial I_b}$	$\frac{\partial WMI}{\partial k}$	$\frac{\partial WMI}{\partial f}$
$\frac{\partial P}{\partial I_p}$	<i>0.789</i>	-0.820	0.877	-0.940
$\frac{\partial P}{\partial I_b}$	-0.605	0.054	-0.571	0.266
$\frac{\partial P}{\partial k}$	0.736	-0.937	<i>0.792</i>	-0.644
$\frac{\partial P}{\partial f}$	-0.468	0.596	-0.853	<i>0.968</i>

Italicized values represent the significant correlations ($p < 5\%$)

Fig. 6 Comparison between sensitivity analysis of *WMI* and *P*



gas metal arc welding process with a set of multiple correlated responses. From the experimental and theoretical results, we draw the following conclusions:

1. For special cases where the first principal component is not enough to represent most of the variation of the welding data set, this work presents a novel alternative index. Called the WMI, it is written in terms of the weighted principal component scores.
2. The similarity to and advantages of the WMI criterion with respect to the desirability index has been showed. In this specific case, WMI was more appropriate for the optimization than was desirability.
3. A framework considering the evaluation of the variance–covariance (or correlation) structure of the response data set was developed. The framework indicated the most adequate multivariate hypothesis tests to be used in optimizing multiple correlated responses.
4. The paper presented indices and tests capable of determining the minimum number of principal components that must be kept to form the multivariate index.
5. A case study was developed on a P-GMAW process optimization problem where just two principal components were responsible for 85.5% of the total variation in a nonlinear model. Experimental results have been shown to be compatible with the theory.
6. ANOVA verifies the adequacy of the full quadratic model, presenting a p value for the lack-of-fit test equals 0.227. Considering the full quadratic model of WMI as a multivariate objective function, the optimal settings for the P-GMAW process were obtained: $I_p=344.9$ A, $I_b=104.5$ A, $k=49.5\%$, and $f=5.9$ m/min.
7. Since the multivariate index written in terms of weighted sum is a quadratic function, the GRG routine was shown to be appropriate for the optimization problem. Perhaps using other agglutination methods, like a geometric mean, would make the genetic algorithm more adequate.
8. A sensitivity analysis of these parameters based on the concept of Lagrange multipliers demonstrated that variation around the optimum is not significant. The variation follows a straight line whose angular coefficient is the value of the shadow price.
9. WMI is postulated to be a representative index of the original set of welding correlated responses. It was thus demonstrated that the sensitivity analysis of the original set corresponds to the WMI sensitivity analysis. The correspondence followed the signal of the correlation between the index and the response. A positive correlation with penetration in particular indicated that a positive increment in WMI also corresponded to a positive increment in penetration. The magnitude of the increment, however, was not the same.

The aforementioned conclusions cannot be extrapolated to different materials, parameters, and designs, and they are only valid in the adopted level range. Nonetheless, the methodology can be recommended to fit any welding processes.

Acknowledgement The authors would like to express their gratitude to FAPEMIG, CAPES, and CNPq for their financial support in this research and would like to thank the anonymous reviewers for their contributions and suggestions.

References

- Wu FC (2005) Optimization of correlated multiple quality characteristics using desirability function. *Qual Eng* 17(1):119–126
- Chiao H, Hamada M (2001) Analyzing experiments with correlated multiple responses. *J Qual Technol* 33(4):451–465
- Box GEP, Hunter WG, MacGregor JF, Erjavec J (1973) Some problems associated with the analysis of multiresponse data. *Technometrics* 15(1):33–51
- Murugan N, Gunaraj V (2005) Prediction and control of weld bead geometry and shape relationships in submerged arc welding of pipes. *J Mater Process Technol* 168:478–487
- Kannan T, Murugan N (2006) Effect of Flux Cored Arc Welding Process parameters on duplex stainless steel clad quality. *J Mater Process Technol* 176:230–239
- Gunaraj V, Murugan N (2000) Prediction and optimization of weld bead volume for the submerged arc process—part 2. *Weld J* 79(11):331–338
- Darwish SM, Al-Dekhial SD (1999) Statistical models for spot welding of commercial aluminum sheets. *Int J Mach Tools Manuf* 39:1589–1610
- Benyounis KY, Olabi AG, Hashmi MSJ (2005) Effects of laser welding parameters on the heat input and weld-bead profile. *J Mater Process Technol* 164–165:978–985
- Vijian P, Arunachalam VP (2007) Modeling and multi objective optimization of LM24 aluminium alloy squeeze cast process parameters using genetic algorithm. *J Mater Process Technol* 186:82–86
- Correia DS, Ferraresi VA (2007) Welding process selection through a double criteria: operational costs and non-quality costs. *J Mater Process Technol* 184:47–55
- Busacca GP, Marseguerra M, Zio E (2001) Multiobjective optimization by genetic algorithms: application to safety systems. *Reliab Eng Syst Saf* 72(1):59–74
- Derringer G, Suich R (1980) Simultaneous optimization of several response variables. *J Qual Technol* 12(4):214–219
- Khuri AI, Conlon M (1981) Simultaneous optimization of multiple responses represented by polynomial regression functions. *Technometrics* 23(4):363–375
- Liao HC (2005) Multi-response optimization using weighted principal components. *Int J Adv Manuf Technol* 27(7):720–725
- Fung CP, Kang PC (2005) Multi-response optimization in friction properties of PBT composites using Taguchi method and principal component analysis. *J Mater Process Technol* 170(3):602–610
- Fung CP (2006) Multi-response optimization of impact performances in fiber-reinforced polybutylene terephthalate. *J Thermoplast Compos Mater* 19(2):191–205
- Tong LI, Wang CH, Chen HC (2005) Optimization of multiple responses using principal component technique for order preference by similarity to ideal solution. *Int J Adv Manuf Technol* 27:407–414
- Yih-Fong T (2007) A hybrid approach to optimize multiple performance characteristics of high-speed computerized numerical control milling tool steels. *Mater Des* 28:36–46
- Bratchell N (1989) Multivariate response surface modeling by principal components analysis. *J Chemom* 3:579–588
- Nian CY, Yang WW, Tarn YS (1999) Optimization of turning operations with multiple performance characteristics. *J Mater Process Technol* 95:90–96
- Montgomery DC (2001) Design and analysis of experiments, 4th edn. Wiley, New York
- Nash SG, Sofer (1996) A linear and nonlinear programming, 1st edn. McGraw-Hill, New York
- Köksoy O, Doganaksoy T (2003) Joint optimization of mean and standard deviation using response surface methods. *J Qual Technol* 35(3):239–252
- Johnson RA, Wichern D (2002) Applied multivariate statistical analysis, 5th edn. Prentice-Hall, New Jersey
- Peres-Neto PR, Jackson DA, Somers KM (2005) How many principal components? Stopping rules for determining the number of non-trivial axes revisited. *Comput Stat Data Anal* 49(4):974–997
- Bartlett MS (1954) A note on the multiplying factor for various χ^2 approximations. *J R Stat Soc* 16:296–298
- Jackson DA (1993) Stopping rules in principal component analysis: a comparison of heuristical and statistical approaches. *Ecology* 74:341–347
- Lawley DN (1956) Test of the significance for the latent roots of covariance and correlation matrices. *Biometrika* 43:128–136
- Todeschini R (1997) Data correlation, number of significant principal components and shape of molecules. The K correlation index. *Anal Chim Acta* 348(1–3):419–430
- Paiva AP, Ferreira JR, Balestrassi PP (2007) A multivariate hybrid approach applied to AISI 52100 hardened steel turning optimization. *J Mater Process Technol* 189:26–35
- Paiva AP, Paiva EJ, Ferreira JR, Balestrassi PP, Costa SC (2009) A multivariate mean square error optimization of AISI 52100 hardened steel turning. *Int J Adv Manuf Technol*. doi:10.1007/s00170-008-1745-5
- Lasdon LS, Jain ADA, Ratner M (1978) Design and testing of a generalized reduced gradient code for nonlinear programming. *ACM Trans Math Softw* 4(1):34–50
- Chen MC, Fan SS (2002) Tolerance evaluation of minimum zone straightness using non-linear programming techniques: a spreadsheet approach. *Comput Ind Eng* 43(3):437–453
- Praveen P, Yarlagadda PKDV, Kang MJ (2005) Advancements in pulsed gas metal arc welding. *J Mater Process Technol* 164–165:1113–1119
- Ghosh PK, Dorn L, Hübner M, Goyal VK (2007) Arc characteristics and behaviour of metal transfer in pulsed current GMA welding of aluminium alloy. *J Mater Process Technol* 94:163–175
- Dorn WS (1961) On Lagrange multipliers and inequalities. *Oper Res* 9(1):95–104
- Karaoğlu S, Seçgin A (2008) Sensitivity analysis of submerged arc welding process parameters. *J Mater Process Technol* 202:500–507
- Sarigül AS, Seçgin A (2004) A study on the application of the acoustic design sensitivity analysis of vibration bodies. *Appl Acoust* 65:1037–1056
- Kim IS, Jeong YJ, Son IJ, Kim IJ, Kim JY, Kim IK, Yaragada PKDV (2003) Sensitivity analysis for process parameters influencing weld quality in robotic GMA welding process. *J Mater Process Technol* 140:676–681
- Kim IS, Son IJ, Yan YS, Yaragada PKDV (2003) Sensitivity analysis for process parameters in GMA welding processes using a factorial design method. *Int J Mach Tools Manuf* 43:763–769
- Myers RH, Montgomery DC (2002) Response surface methodology—process and product optimization using designed experiments (2nd ed.), John Wiley & Sons